Nucl. Geophys. Vol. 7, No. 2, pp. 241–267, 1993
Printed in Great Britain.

0886-0130/93 $6.00+0.00

Development of the Monte Carlo–Library Least-Squares Method of Analysis for Neutron Capture Prompt Gamma-ray Analyzers

C. M. SHYU,* R. P. GARDNER and K. VERGHESE

Center for Engineering Applications of Radioisotopes, Department of Nuclear Engineering, Box 7909, North Carolina State University, Raleigh, NC 27695-7909, U.S.A.

Abstract—A new analysis principle called the Monte Carlo–Library Least-Squares (MCLLS) principle has been identified and investigated in a preliminary way for neutron capture prompt gamma-ray (NCPGR) analyzers. In order to apply the MCLLS method to obtain sample elemental concentrations, the elemental library spectra of the sample elements are required. To accomplish this, an existing Monte Carlo model which simulates the analysis of coal on a conveyor belt using ^{252}Cf and a Ge detector has been modified to predict these elemental library spectra. This Monte Carlo model includes several very efficient variance reduction techniques such as: (1) use of either expected value technique or discrete importance function to determine the interaction type, (2) forcing all prompt γ-rays to be emitted after an (n,γ) event has occurred, (3) use of the direction biasing technique to bias the emitting or scattering direction of primary and secondary photons towards the detector, (4) use of both deterministic estimator and statistical estimator to compute the unscattered detection probabilities of the primary photons and the subsequent secondary photons, (5) use of the correlated sampling method in order to study the sensitivity of the library spectrum shape to sample composition, and (6) use of the detailed detector response function to transform the detected photon spectra to pulse-height spectra. The pulse-height spectra for each element in the sample is stored separately to provide the library spectrum for each element. By studying with the simulated spectra, the MCLLS method appears to be feasible for a good initial guess of the sample composition; furthermore, the proposed iterative MCLLS algorithm works for poor initial guesses of the major element amounts. Testing of the proposed algorithm on the experimental spectrum showed that for the practical application of the iterative MCLLS method certain guidelines should be used. These are provided in the paper. The major problems with the application of MCLLS and their possible solutions are also discussed.

1. INTRODUCTION

The traditional methods for measuring the composition of coal involve laboratory analysis of samples weighing of the order of 1 g. Not only is this process slow, tedious and expensive if simulating continuous sampling, but also the inhomogeneous nature of coal results in the average compositions of the small samples not being representative of the bulk material. Therefore, a need exists for an instrument which can determine on an "on-line" basis the amounts of the major elements in bulk materials such as coal. The analysis should be performed continuously and automatically on samples which represent significant fractions of mass flow rates that may exceed several hundred tons per hour.

A technique known as PGNAA (Prompt Gamma Neutron Activation Analysis) is used to measure raw material elemental composition. The use of PGNAA in multielement sample analysis has greatly increased during the past few years. Extensive experimental studies have been done in bulk coal analysis (Gozani *et al.*, 1977, 1978; Duffey *et al.*, 1978; Reynolds *et al.*, 1979; Marshall and Zumberge, 1989). In all these applications the detected γ-ray intensities from the elements present are used to estimate their concentrations. The PGNAA phenomenon is based on the radiative capture reaction between a neutron and the nucleus of any atom. The problems associated with

* Present address: GAMMA-METRICS, 5788 Pacific Center Blvd, San Diego, CA 92121, U.S.A.

the application of PGNAA for bulk analysis (including coal analysis) stem primarily from the highly nonlinear nature of the γ-ray response of each element. The γ-ray intensities from each element are functions of the concentrations of all the elements present and of several other sample matrix parameters such as bulk density, moisture and temperature. A change in any of these parameters alters the measured γ-ray intensities. Therefore, analyzers must be extensively calibrated as a function of all these parameters in order to extract information about the concentration of specific elements from measured spectra. Calibration can be accomplished empirically by laboratory experimentation. For the analysis of complex matrices such as coal, this implies the need for a very large set of bulk samples of known concentrations and other parameters which must be measured with the analyzer of interest. An accurate computational model allows one to augment or, in many cases, to essentially replace the experimental measurements necessary in analyzer calibration. Such a model also facilitates the design optimization of these analyzers, and can also be used to determine analysis sensitivity for any element in any sample of interest.

2. OVERVIEW OF THE MONTE CARLO–LIBRARY LEAST-SQUARES METHOD

2.1. *Monte Carlo–Library Least-Squares (MCLLS) method*

While it is possible to use only the signals from the uncollided prompt γ-rays (those that have not interacted at all in the sample) which deposit all of their energy in the detector, this approach has a number of disadvantages; all available information is not used and particularly when sodium iodide detectors are used, the peaks in the spectrum overlap and it is often difficult to separate the γ-ray peaks from the different elements. Presently accepted industrial practice is to use some form of the library least-squares approach of spectral analysis which is capable of using all of the spectral information that is available. This approach consists of formulating the problem of determining individual elemental γ-ray spectral intensities into a linear combination of those from all elements present.

If y_i is the counting rate in counts/s in channel i of the γ-ray spectrum from the sample of interest, then it can be represented as

$$y_i = \sum_{j=1}^{m} x_j a_{ij} + e_i \text{ counts/s} \qquad \text{for} \quad i = 1, \ldots, n \tag{1}$$

where x_j is the amount of element j present in atom density units (atoms/cm^3), a_{ij} is the "library" spectrum of element j in counts/s in channel i per unit atom density of that element (counts/s per atoms/cm^3), and e_i is the random error in channel i due to statistical counting rate fluctuations (counts/s). This is a linear problem that can often be solved for x_j by first forming the sum of the squares of the e_i over all channels. Or, more exactly, the reduced chi-square is formed by

$$\chi_v^2 = \sum_{i=1}^{n} e_i^2 / v\sigma_i^2 \tag{2}$$

where σ_i is the standard deviation (or expected deviation) of e_i and v is the number of degrees of freedom given by $n-m-l$. The values of x_j can be obtained by minimizing χ_v^2 with respect to each x_j, which involves setting the first derivative of χ_v^2 with respect to each x_j equal to zero. This yields a set of m linear simultaneous equations that can be solved directly for the x_j amounts.

This method has been applied to energy-dispersive x-ray fluorescence (EDXRF) analyzers to analyze the Cu–Ni alloy (Shyu *et al.*, 1988) and the agreement of calculated composition with the actual composition of the sample is excellent. Unfortunately, there are several practical difficulties in the application of this approach to the coal analysis problem. First of all, the library least-squares method is a linear representation which strictly applies to the present nonlinear problem only when a linear approximation is valid. For example, this would be the case when the library spectra (a_{ij})

are obtained for samples with x_j very close to those in the unknown sample of interest. Both the library intensities and shapes are affected by sample composition. Secondly, it is very difficult, if not impossible, to experimentally determine accurate library spectra even when the restriction of the x_j being close to those of the sample of interest is relaxed. Finally, the counting rates usually employed in this application are quite high so that adequate accuracy is obtained in measurement times consistent with continuous on-line measurement. This causes spectral distortions due to pulse pile up which adds an additional nonlinear problem.

If the spectral shapes of the elemental library spectra remained constant, independent of sample elemental composition, these problems could be solved by the combination of a relatively simple experimental approach in which the shapes of individual elemental library spectra are obtained from the "spiking" of mixtures of simple organic materials (like wax or plastic powders) and their intensities are obtained from measurement of samples of known composition close to the sample composition of interest. Even if this were the case, the experimental effort involved in accumulating, storing and using many well characterized samples of known composition requires a very extensive experimental effort (Marshall and Zumberge, 1989). This approach with adjustable parameters to take care of the limited number of calibration samples that were used, and indirectly, the effect of changing library spectral shapes has apparently been used in various forms by the commercial suppliers.

This leads to consideration of the principle described and tested in a preliminary way here—the Monte Carlo–Library Least-Squares (MCLLS) principle. In this approach Monte Carlo simulation is used to generate the elemental library spectra, thus eliminating the need for an elaborate and extensive experimental program and, perhaps more importantly, taking care of the fundamental problem of library spectral shape variation with sample composition.

The MCLLS principle is applied to PGNAA by the following steps.

1. Generate the complete spectra response for a sample of known assumed composition by Monte Carlo simulation. This assumes that a very accurate Monte Carlo code exists that describes the application in detail.
2. Within the Monte Carlo code, arrange to keep track (this is just a bookkeeping problem) of the individual spectral response for each element within the sample to provide the necessary library spectra (a_{ij}).
3. Use the linear library least-squares analysis method to obtain the elemental amounts (x_j) in any unknown sample or samples for which the complete spectral response (y_i) has been measured.
4. If the calculated elemental amounts (x_j) for the unknown sample are not close enough to those originally assumed for the Monte Carlo calculation so that a linear relationship exists, then another iteration of these steps is necessary by starting with an assumed sample composition closer to that of the unknown sample.

2.2. Description of configuration modeled

The modeling configuration is a static system resembling the on-line systems which are now commercially available except for the type of detector. The experimental arrangement for bulk coal treated here consists of a 2 μg sealed ^{252}Cf neutron source placed on one side of a rectangular sample box and a 39% high-purity Ge detector, which has an active volume of 170 cm^3, placed on the other side. The neutron source is shielded with lead to minimize the detection of fission γ-rays. A neutron shield consisting of paraffin and lithium is located around the neutron source to reduce neutron exposure to personnel. The detector is shielded with lithiated paraffin to prevent neutron damage. The dimensions and geometrical arrangement are shown in Fig. 1.

2.3. Compositions of measured coal samples

Four coal samples of different compositions are tested. Tabulated in Table 1 are the compositions

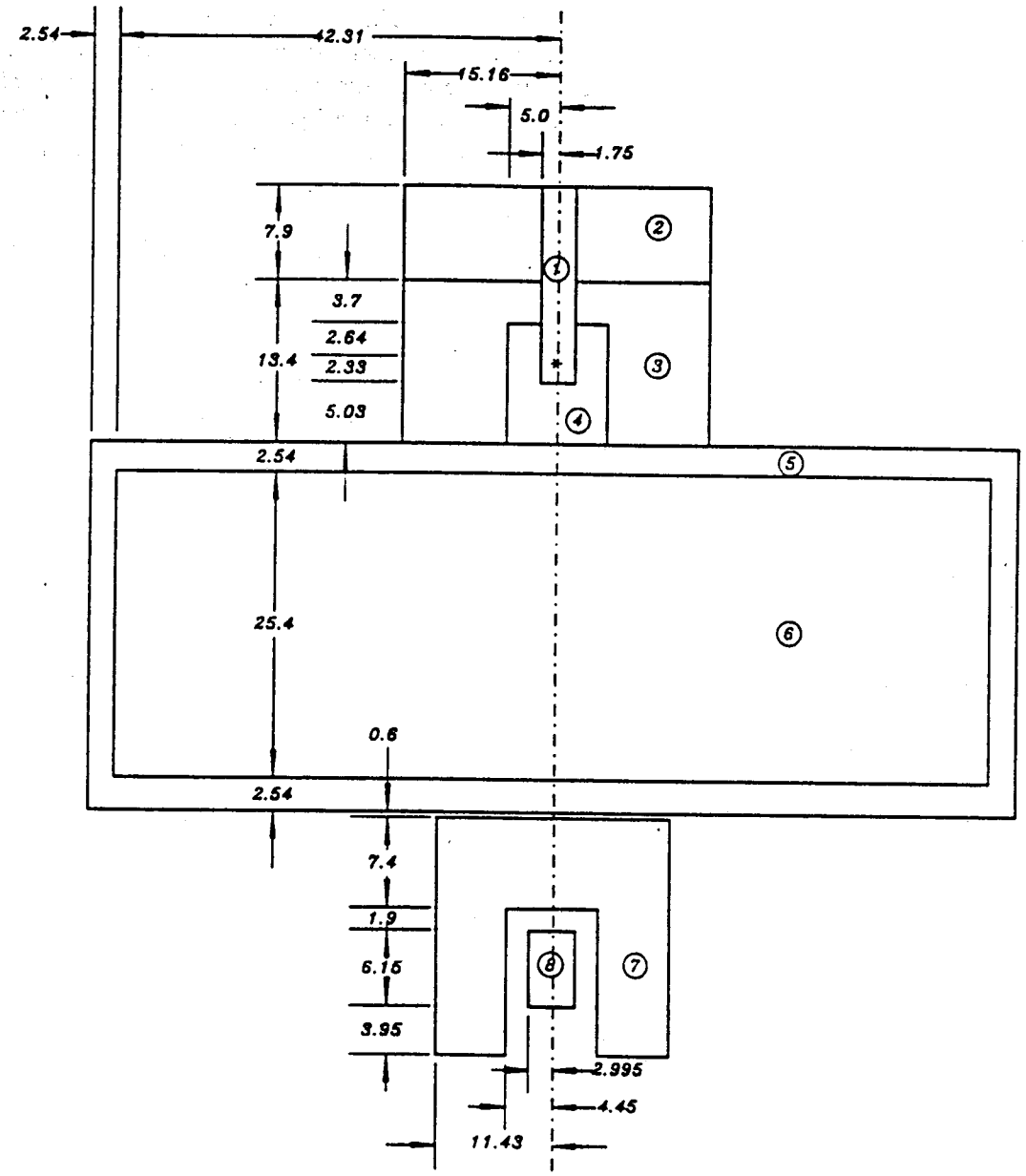

Fig. 1. Experimental configuration for bulk coal analysis. 1, Polypropylene; 2, paraffin wax; 3, paraffin wax and lithium carbonate; 4, lead; 5, polyethylene; 6, coal; 7, paraffin wax and lithium carbonate; 8, NaI(Tl) detector. * Neutron source.

of the major* and minor elements obtained by neutron activation analysis (Weaver, 1989), and the compositions determined by chemical ultimate analysis (Huffman Laboratory, 1988) are given in Table 2. After adding the appropriate amount of moisture, which is lost during the drying process, and normalizing to 100%, the resulting adjusted compositions used in the present work are tabulated in Table 3.

2.4. *Compositions of simulated coal samples*

The correlated sampling method (Gardner *et al.*, 1990), which is described in detail in section 3.7, is used to predict the detector responses for different sample densities and/or compositions within

*The major elements means those with considerable contribution to either neutron macroscopic sections or photon attenuation coefficients of the sample.

Table 1. Elemental composition* of coal sample I, II, III and IV by neutron activation analysis

Element	Sample I	Sample II	Sample III	Sample IV
Tl	615.5±16.1%	536.15±18.4%	548.66±17.2%	676.31±16.1%
Sn	<4.6	<5.0	<5.0	<5.0
I	<0.21	<0.30	<0.25	<0.20
Mn	27.747±2.4%	29.729±2.4%	11±5.6%	21.041±3.6%
Mg	580.35±15.8%	468.74±17.4%	438.92±23.6%	447.33±24.4%
Cu	<50.0	<50.0	<50.0	<50.0
V	17.009±4.2%	47.731±1.9%	16.436±6.1%	52.9±1.6%
Cl	174.82±14.6%	1250.82±5.2%	441.89±11.2%	2792.08±3.0%
Al	8940.75±0.7%	9047.93±0.7%	11831.14±0.7%	9864.3±0.7%
Hg	<0.10	<0.10	<0.10	<0.10
Sm	0.823±0.7%	0.657±0.7%	1.107±0.5%	0.808±0.7%
W	<2.0	<2.0	<2.0	<2.0
Mo	12.584±3.9%	15.891±6.0%	<0.5	11.397±8.5%
U	2.434±7.1%	2.574±7.2%	1.041±15.3%	1.765±9.5%
La	4.965±2.9%	4.661±3.0%	8.91±1.9%	5.545±3.2%
Cd	<0.55	<0.50	<0.61	<0.47
As	1.807±6.3%	3.49±3.8%	1.888±7.4%	3.215±6.9%
Sb	0.773±2.7%	1.538±1.6%	0.439±4.7%	1.684±1.7%
Zr	<7.3	15.696±17.5%	<7.0	9.304±19.2%
Br	1.83±11.2%	10.124±1.5%	8.984±2.5%	25.448±1.1%
Na	251.65±3.0%	336.93±2.5%	127.89±5.7%	346.57±2.8%
K	2750.82±18.1%	1240.98±21.9%	480.33±26.1%	3357.38±15.8%
Ce	12.259±1.3%	9.086±1.5%	14.139±1.5%	9.31±1.5%
Lu	0.074±8.6%	0.072±6.9%	0.087±6.9%	0.068±8.0%
Eu	0.162±16.3%	0.161±17.0%	0.275±10.1%	0.178±14.6%
Se	2±17.4%	3.461±10.2%	5.639±6.7%	3.276±9.1%
Tb	0.122±7.2%	0.116±7.5%	0.2±4.3%	0.134±5.7%
Th	1.221±1.8%	1.159±1.7%	1.62±1.3%	1.351±1.4%
Cr	13.628±2.1%	13.828±1.9%	11.446±2.4%	13.929±1.6%
Yb	0.157±18.1%	0.125±19.3%	0.455±13.0%	0.133±19.0%
Hf	0.467±9.9%	0.451±6.0%	0.544±9.0%	0.503±5.2%
Ba	55.611±18.1%	57.796±18.0%	73.241±14.7%	96.407±10.2%
Nd	6.83±14.5%	4.274±15.9%	2.306±18.3%	5.224±14.9%
Cs	1.025±9.3%	0.793±9.2%	0.634±9.8%	0.856±7.4%
Ag	1.364±16.9%	4.577±5.4%	16.445±1.8%	0.427±15.8%
Ni	<0.21	3.431±16.9%	12.719±6.2%	9.194±8.0%
Sc	2.204±0.3%	1.662±0.3%	2.438±0.3%	1.943±0.4%
Rb	0.424±13.9%	0.436±12.2%	0.278±16.0%	0.403±10.4%
Fe	13641±0.4%	13624.34±0.5%	1769.4±2.6%	9074.06±0.6%
Zn	<50.0	<50.0	<50.0	<50.0
Co	2.811±2.1%	2.817±1.8%	10.912±0.8%	2.049±1.7%

* Unit: micrograms element/gram matrix.

Table 2. Elemental composition of coal sample I, II, III and IV by chemical ultimate analysis

Element	Sample I (%)	Sample II (%)	Sample III (%)	Sample IV (%)
Dry-loss*	9.32	9.34	7.14	7.22
C	71.63	71.58	77.02	76.11
H	5.16	5.20	5.21	5.28
O	10.71	10.44	9.88	8.39
N	1.45	1.42	1.47	1.60
S	3.82	3.45	0.77	2.78
Ash	9.30	9.32	6.39	8.91

* The loss on drying was performed at 105°C in air for 1 h and is on an as received basis. All of the other results are on a dried basis.

one Monte Carlo simulation. The sample compositions used for simulation include the four given in Table 3 with Sample I used as the *reference sample*. The other three samples in Table 3, together with 57 other different samples, obtained by changing only density or atom density of only one element from the *reference sample*, are used as the *comparison samples*, where the *reference sample* and the *comparison samples* are defined in section 3.7. The variations made to get the *comparison*

Table 3. Adjusted elemental composition* of coal samples used in experiments

Element	Sample I	Sample II	Sample III	Sample IV
H	5.62700%	5.69400%	5.60100%	5.56100%
C	63.63700%	63.99200%	70.99500%	68.51200%
N	1.28800%	1.28690%	1.35500%	1.44000%
O	17.79200%	17.62800%	15.44800%	13.96400%
Na	0.02282%	0.03055%	0.01188%	0.03215%
Mg	0.05263%	0.04250%	0.04076%	0.04150%
Al	0.81070%	0.82030%	1.09860%	0.91520%
Si†	2.60000%	2.60000%	2.60000%	2.60000%
S	3.39400%	3.08400%	0.70980%	2.50200%
Cl	0.01585%	0.11340%	0.04103%	0.25905%
K	0.24940%	0.11250%	0.04460%	0.31150%
Ca†	3.21655%	3.32869%	1.83802%	2.95566%
Ti	0.05581%	0.04861%	0.05095%	0.06275%
Cr	0.00124%	0.00125%	0.00106%	0.00129%
Fe	1.23700%	1.23520%	0.16430%	0.84190%
Density (g/cm^3)	0.67552	0.60209	0.79314	0.88169

*Fractions listed in this table are in weight percent.
†The amounts of Si and Ca are assumed amounts.

Table 4. Composition of coal samples used in simulation*

Sample No.	Variation	Sample No.	Variation	Sample No.	Variation
No. 2	density(+5%)†	No. 22	Mg(+50%)	No. 41	K(+10%)
No. 3	density(−5%)	No. 23	Mg(−50%)	No. 42	K(−10%)
No. 4	H(+1%)‡	No. 24	Mg(+100%)	No. 43	K(+50%)
No. 5	H(−1%)	No. 25	Al(+10%)	No. 44	K(−50%)
No. 6	H(+5%)	No. 26	Al(−10%)	No. 45	Ca(+10%)
No. 7	H(−5%)	No. 27	Al(+30%)	No. 46	Ca(−10%)
No. 8	C(+1%)	No. 28	Al(−30%)	No. 47	Ca(+50%)
No. 9	C(−1%)	No. 29	Si(+50%)	No. 48	Ca(−50%)
No. 10	C(+5%)	No. 30	Si(−50%)	No. 49	Ti(+10%)
No. 11	C(−5%)	No. 31	S(+10%)	No. 50	Ti(−10%)
No. 12	N(+1%)	No. 32	S(−10%)	No. 51	Ti(+50%)
No. 13	N(−1%)	No. 33	S(+20%)	No. 52	Ti(−50%)
No. 14	N(+5%)	No. 34	S(−20%)	No. 53	Cr(+50%)
No. 15	N(−5%)	No. 35	S(+50%)	No. 54	Cr(−50%)
No. 16	O(+10%)	No. 36	S(−50%)	No. 55	Fe(+10%)
No. 17	O(−10%)	No. 37	Cl(+50%)	No. 56	Fe(−10%)
No. 18	Na(+1%)	No. 38	Cl(−50%)	No. 57	Fe(+30%)
No. 19	Na(−1%)	No. 39	Cl(+100%)	No. 58	Fe(−30%)
No. 20	Na(+5%)	No. 40	Cl(+500%)	No. 59	Sample II§
No. 21	Na(−5%)			No. 60	Sample III
				No. 61	Sample IV

*Sample I on Table 3 is used as the reference sample, sample No. 1.
†Means increasing the density of Sample No. 1 by 5%.
‡Means increasing the atom density of H of Sample No. 1 by 1%.
§These are the sample compositions given in Table 3.

sample compositions are listed in Table 4. It is obvious that the change of the atom density of a single element while keeping that of the other elements the same will result in the change of weight fractions of all elements as well as the sample density.

3. VARIANCE REDUCTION TECHNIQUES

The main drawback of the Monte Carlo method is that it is often too expensive to do many calculations of interest. This is not because the method is slow, but because a great deal of

computational time can be wasted following unimportant or statistically insignificant events to achieve a desired result. Thus, the key to making the Monte Carlo method attractive is to somehow concentrate on important aspects of a given problem without wasting time on the unimportant ones. The schemes, called "variance reduction techniques", that do this can be looked at as increasing the computational efficiency or convergence rate for a given solution accuracy. The variance reduction techniques used in this work are described in the following sections.

3.1. Russian Roulette

The Russian Roulette method is used in conjunction with the expected value technique, which is described in detail in section 3.5, to randomly terminate the neutron history or photon-tracking process when its weight falls below a preassigned value, w_{min}. If the particle weight is less than w_{min}, a random number ξ, between 0 and 1, is sampled and compared to the ratio of the particle weight to w_{min}. The particle survives and its weight is raised from w to w_{min} if $\xi \leqslant w/w_{min}$; otherwise, the neutron history or photon-tracking process is terminated.

3.2. Truncated exponential pdf

Having established the distance D to the boundary in the particle direction of flight, the distance d to interaction is determined. If the particle will not reenter the system once it leaves the boundary of present interest, the particle is mostly not allowed to escape this boundary* and the distance d to an interaction is sampled from the truncated exponential probability density function (pdf). If the boundary of interest is not part of the system boundary or the particle might reenter the system after it leaves the present boundary, then the distance d to an interaction is sampled from an unbiased exponential pdf.

3.3. Direction biasing

The direction biasing technique is applied from sampling the photon direction. Suppose a predefined direction (u, v, w) and the true pdf $f(\nu)$, with μ being the cosine of the angle between the predefined direction and the sampled new direction, are given. Instead of sampling from the true pdf $f(\nu)$, $\mu \in [-1, 1]$, μ is sampled from a fictitious pdf $f(\nu)$. By changing the variable $x = 1 - \mu$, the transformed fictitious pdf $g'(x)$, $g'(x) = f(\nu)$, has the form of

$$g'(x) = ae^{-bx}, \qquad \text{for} \quad 0 \leqslant x \leqslant 2. \tag{3}$$

By normalizing the transformed fictitious pdf $g(x)$ in equation (3), we have $a = b/[1 - \exp(-2b)]$. With the sampled random number ξ, between 0 and 1, solving

$$\xi = \int_0^x g'(x')\mathrm{d}x', \tag{4}$$

the sampled μ is

$$\mu = -\frac{1}{b}\ln[1 - \xi(1 - e^{-2b})], \tag{5}$$

and the adjusting weight of this biased sampling is $w_{adj} = f(\mu)/f'(\mu)$.

3.3.1. For primary photons. For the primary photons, which are those emitted directly from fission, inelastic scattering, or radiative capture, the predefined direction (u, v, w) in section 3.3 is defined to be the direction from the present position to the center of the detector. Since the primary photons are emitted isotropically (Gardner and Verghese, 1971), the true pdf $f(\nu)$ in this case would

* If the particle is not within the vacuum zone before meeting the system boundary, the particle is forced to have an interaction within this zone; otherwise, the particle will be allowed to escape from the system.

be $f(v)=1/2$, for $v\in[-1,1]$. In conjunction with the fictitious pdf given in equation (3), this sampling is biasing the primary photons emitted toward the detector. The adjusting weight associated with this sampling is $w_{adj}=1/[2f'(\mu)]$.

3.3.2. For secondary photons. For the secondary photons, which are those after Compton scattering, the predefined direction (u, v, w) in section 3.3 is defined to be the initial photon direction of flight before Compton scattering. In conjunction with the fictitious pdf given in equation (3), this biased sampling is enhanced in the forward direction. Furthermore, since its primary photon emitting direction is biased toward the center of the detector, this sampling biases the secondary photon scattered toward the detector as well. The true pdf $f(v)$ for the photons having a Compton scattering interaction can be obtained by normalizing the Klein–Nishina differential scattering cross section.

3.4. *Discrete importance function*

The importance sampling (Carter and Cashwell, 1975) applied to a discrete pdf can be described as follows: Suppose $E_1,\ldots,E_n$ are n independent, mutually exclusive events with probabilities $p_1,\ldots,p_n$, respectively, $p_1+\ldots+p_n=1$. A discrete importance function defines I_i for the importance of the event E_i. Then the fictitious discrete pdf becomes

$$p_i'=\frac{I_i p_i}{C}, \qquad \text{for} \quad i=1,\ldots,n, \tag{6}$$

where

$$C=\sum_{i=1}^{n} I_i P_i. \tag{7}$$

If a random number ξ, $0\leqslant\xi\leqslant 1$, is such that $p_1'+\ldots+p_{i-1}'\leqslant\xi<p_1'+\ldots+p_i'$, then ξ determines the event E_i. The adjusting weight corresponding to this sampled even would be $W_{adj}=p_i/p'=C/I_i$.

The importance constants I_i should always be greater than or equal to zero, and zero importance is equivalent to forcing the corresponding event not to occur. Choosing all I_i the same means sampling from the true discrete pdf without introducing biasing.

3.5. *Expected value technique (EVT)*

Suppose $E_1,\ldots,E_n$ are n independent, mutually exclusive events with probabilities $p_1,\ldots,p_n$, respectively, $p_1+\ldots+p_n=1$. Clearly, if a random number ξ, $0\leqslant\xi<1$, is such that $p_1+\ldots+p_{i-1}\leqslant\xi<p_1+\ldots p_i$, then ξ determines the event E_i. This random process, referred to as direct sampling, inevitably results in some statistical fluctuations. Assuming the cumulative weight at the present point is W_0, the expected value technique (McGrath and Irving, 1975) can be employed by starting n independent random walks from this point with the starting weight $W_i=p_i W_0$, for $i=1,\ldots,n$, respectively. The EVT is used in determining interaction type, in determining element of interaction, and in determining emitted prompt γ-ray energy.

3.6. *Unscattered detection probability estimator*

The expected value of the unscattered detection probability of a photon, which is either emitted from fission, from inelastic scattering, from radiative capture or scattered from Compton scattering, is

$$P=\int_{v_{min}}^{v_{max}}\int_{\rho_{min}(v)}^{\rho_{max}(v)} p_1(v,\rho)\times p_2(v,\rho)\times p_3(v,\rho)\,d\rho\,dv, \tag{8}$$

where

$p_1(v,\rho)$ = the probability of scattering or emitting toward the detector through the angles (v,ρ)*;

$$p_2(v,\rho)=\exp\left[-\sum_{i=1}^{n}\mu_i l_i(v,\rho)\right],$$

= the probability that the photon will be transmitted to the detector with the direction angles (v,ρ) without collision, with μ_i and l_i being the linear attenuation coefficient of zone i and path length through zone i, respectively;

$$p_3(v,\rho)=1-\exp[-\mu_D l_D(v,\rho)],$$

= the detection probability with μ_D and l_D being the linear attenuation coefficient and path length in the detector, respectively.

Most Monte Carlo codes (Yuan *et al.*, 1987) use the statistical estimator to approximate the integration in equation (8). Yakowitz (1977) suggested that quadrature methods should be used for well-behaved real functions. Both deterministic and statistical estimators, described in detail in sections 3.6.1 and 3.6.2, respectively, are used in the present work.

3.6.1. Deterministic estimator. The double integral in equation (8) can be approximated by numerical integration methods, for example, the trapezoidal rule or quadratures, which are more accurate but computationally expensive. This method is preferred for scoring the unscattered primary photons from fission, from inealstic scattering, and from radiative capture reactions, since the energy of the scored photon is independent of the directions determined by quadratures. But it is difficult to apply this method to score the secondary photon from Compton scattering since the energy of the scored photon is a function of the angle between the incident photon direction and the directions determined by quadratures.

3.6.2. Statistical estimator. The double integral in equation (8) can also be estimated by sampling a direction toward the detector and the estimated probability is the integrand evaluated at the sampled direction. This method is cheaper than the deterministic estimator, but much less accurate. this estimator is used for scoring the secondary photon from Compton scattering.

3.7. Correlated sampling

The correlated sampling method is used to predict the change in the detector response due to changes in the sample zone density and/or compositions. It can be used to predict the relative changes in the elemental library spectra due to small changes in the coal composition. This is an excellent way to investigate the spectral changes due to small variations in composition. Without it, the relative change in the simulated detector response will be lost in the Monte Carlo "variance".

To illustrate the basic principle of correlated sampling, let us consider two measuring systems with identical geometry but different sample compositions†. We can start two completely independent simulations for these two systems with similar random walk sampling schemes, i.e. starting at the same source position, considering the same interactions, scoring the same information, etc. Either of these two simulations ordinarily would use the pdf's determined by its own sample composition when the random walks pass through or have interactions within the sample. Alternatively, instead of sampling according to the pdf's determined by its own sample composition, the random walks can proceed according to the pdf's determined by the sample composition of the other system. These pdf's can be thought as the fictitious pdf's in the importance sampling

* The angles (v,ρ) represent the direction determined by the polar angle $\cos^{-1}(v)$ and the azimuthal angle ρ.
† In general, correlated sampling can be applied to a system with different composition for more than one zone.

method, thus appropriate weight adjustment should be made to ensure the correct expected results. Define one sample of these two systems as the *reference sample*, and the sample of the other system as the *comparison sample*. The correlated sampling method thus can be performed by combining these two independent simulations into one with all the random walks based on the pdf's determined by the *reference sample* composition when they pass through or have interactions within the sample.

The important regions of phase space in the two samples might shift a lot if the *reference sample* and the *comparison sample* have very different compositions. In this case, a larger number of histories are necessary to ensure that the results are converging to the correct results for both *reference sample* and *comparison sample*, respectively.

Consider one comparison sample in applying the correlated sampling method*. The weight ratio r_c, which is the ratio of the weight of the *comparison sample* to that of the *reference sample*, is initialized to be unity at the beginning of each history. As the sampling related to the composition of the sample is carried out during the history, r_c is modified by multiplying the adjusting weight

$$W_{adj}^{c}(\tilde{z}) = \frac{P_c(\tilde{z})}{P_r(\tilde{z})}, \tag{9}$$

where $P_c(\tilde{z})$ and $P_r(\tilde{z})$ are the pdf's of the *comparison sample* and of the *reference sample* evaluated at the sampled random variable $\tilde{z}$, which is sampled based on the pdf $P_r(z)$. The response ("absolute" weight) of the *comparison sample* can be obtained any time during the simulation by multiplying that of the *reference sample* by the cumulative weight ratio, r_c. There are three things should be noticed:

1. The cumulative weight ratio r_c needs to be modified only when the pdf, $P_r(z)$ is dependent on the sample composition.
2. As long as the pdf, $P_r(z)$, is dependent on the sample composition, the cumulative weight ratio r_c should be modified according to equation (9) no matter whether the random variable $\tilde{z}$ is determined by a sampling or a forcing scheme.
3. The *reference sample* should contain all the elements in the *comparison sample*, while the *comparison sample* may have some elements absent from the *reference sample*. This is the major restriction of the correlated sampling method.

The details of how to apply equation (9) in (1) sampling particle path length to next collision, (2) sampling interaction type, (3) sampling collision element, as well as in scoring the unscattered photon weights detected, are illustrated in a paper by Gardner *et al.* (1990), which also describes the way of estimating the detector responses and calculating the standard deviations of the *comparison samples*.

It is worth mentioning that the detector response differences and their variances between the *reference sample* and the *comparison samples* could be computed during the simulation. Afterwards, the experimental measured detector response of the *reference sample* could be used together with these computed detector response differences to predict the detector responses of the *comparison samples*. The detailed description of how to calculate the detector response differences and their variances can be found in that paper, too.

4. CROSS SECTIONS

4.1. Neutron cross sections

The neutron interactions considered in this work are elastic scattering, radiative capture, inelastic scattering of carbon and lead, the (n,α) reaction of ^{6}Li, and the (n,p) reaction of ^{14}N. Neutron

* It is very easy to extend the consideration to more than one *comparison sample*.

cross section data are based on ENDF/B-V pointwise data, which cover the energy range of 10^{-5} eV to 20 MeV for all elements at 300 K. These are free atom cross sections which differ from bound atom cross sections by the reduced mass effect. The scattering cross section of bound atoms is proportional to the square of the reduced mass of the neutron–nucleus system. For heavy atoms the reduced mass is practically equal to the neutron mass, hence the ratio of the scattering cross section for the bound atom to the free atom is essentially unity. Nevertheless, for the lightest atom, hydrogen, this reduced effect is most prominent. Therefore, in this work, the scattering cross section data for all bound hydrogen at neutron energies <2 eV are based on experimental data for water at 296 K (Beyster *et al.*, 1965). The scattering cross sections of hydrogen bound in polyethylene (Armstrong, 1965) and in paraffin wax (Rainwater *et al.*, 1948) are almost the same as in water. It is appropriate to neglect anisotropic scattering in the COM system except the anisotropy of the elastically scattered neutrons in lead (Yuan *et al.*, 1987). The angular distributions for elastic scattering are given as Legendre polynomial coefficients, and they are given in the COM system in File 4 of ENDF/B-V. An interpolation scheme, in which each coefficient is linear in neutron energy, is used to obtain coefficients at intermediate neutron energies (Kinsey, 1979). Another simplified sampling scheme, suggested by Yuan *et al.* (1987), is used in the present work.

4.2. Photon cross sections

Photon cross section data is based on the compilation of Storm and Israel (1967). These data were also fitted by the cubic spline method, but on linear scales instead of logarithmic scales because the photon energy range of interest is narrow (1–12 MeV) compared to that for the neutrons and the photon cross sections are a smoothly varying function of energy for a range of two decades. Photon cross sections calculated from linear scales are not much different from those calculated from logarithmic scales. This method also reduces the computing time for cross sections compared to log interpolation even though the number of data points is <10.

5. SAMPLING SCHEMES FOR PARTICLE TRANSPORT

The key ingredient of the MCLLS scheme is the ability to accurately simulate the spectral response of the coal analyzer system. Monte Carlo simulation accuracy is dependent not only on the accuracy of the physical models of radiation transport, but also on the ability to reduce the variance in the simulated results through the use of efficient variance reduction methods. In this section, the Monte Carlo simulation scheme is described, most of which is of a generic nature. The original code was written by Jin *et al.* (1987), and $>95\%$ of that code has been rewritten. The enhancements are listed below:

1. Use more condensed arrays so that the code can handle larger scale problems, such as more elements in the sample, prompt γ-rays, or more comparison samples.
2. Employ other variance reduction techniques, including direction biasing, discrete importance function, deterministic estimator, (new) statistical estimator and correlated sampling.
3. Categorize the scored photon weights in such a way as to get the required (elemental) library spectra.
4. Use more general geometry tracking subroutines to simulate more complicated geometry, which consists of zones surrounded by planes in any direction and cylinders in one direction (z-direction). This code has a version using another even more general geometry tracking module named HERMETOR (Prettyman, 1990).
5. A version has been tested on a parallel machine (CRAY Y/MP).

Each neutron history is initiated by sampling the source parameter. The neutron is then tracked through the various shielding components as well as through the medium. Since the fission γ-ray spectrum converges much faster than the inelastic scattering γ-ray spectrum and the prompt γ-ray spectrum, the fission γ-rays are tracked for every 10 neutron histories by multiplying its initial weight by 10. Since the inelastic scattering cross section is very low compared with the elastic cross section, to reduce the variance of inelastic scattering emitted photon weight, this reaction is forced to occur first whenever its cross section is nonzero, then the neutron history is continued by properly adjusting its weight, until *terminating* radiative capture occurs or the neutron is killed by Russian Roulette. It is found in the crude Monte Carlo simulation that only about 8% of the neutron histories is terminated by radiative capture within the sample zone. To get more complete information from the sample zone as well as from the *extraneous zone*, when the tracked neutron is successfully thermalized and has an interaction within the sample zone, the radiative capture is first forced to occur to score all the prompt γ-rays information, then the neutron is retracked to its next interaction site, by properly adjusting its weight. Then another radiative capture is forced to occur in a similar way. This forcing procedure continues until information from 10 radiative capture events is scored, then the sampling procedure is employed again. The forced radiative capture events are referred to as the *surviving* radiative capture since the neutron tracking continues after the prompt photon tracking. The sampled radiative capture events are referred as the *terminating* radiative capture since the neutron history will be terminated after tracking all the emitted prompt γ-rays. Interactions are forced to occur within the system boundary for both neutron and photon tracking. Each neutron is tracked until a *terminating* radiative capture interaction occurs or it is killed by Russian Roulette. When a radiative capture event initiates, either a *surviving* or *terminating* radiative capture event, all the prompt γ-rays from each element are forced to be emitted and are tracked individually.

Three kinds of primary photon sources are considered, including the fission emitted photons, the inelastic scattering emitted photons, and the radiative capture emitted photons. For these primary photons, the weights of transmission through the medium without having interactions and interacting within the detector are computed by the *deterministic estimator*, section 3.6.1, and scored. Then the primary photons are retracked by sampling its emitting direction, sampling the path length to the next collision, and forcing Compton scattering to occur. The Compton scattered photons are referred to as the *secondary* photon sources. For these secondary photons, the weights of transmission through the medium without having interactions and interacting within the detector are computed by the *statistical estimator*, section 3.6.2, and scored. Then this secondary photon is retracked in a similar way to get the next secondary photon. The photon-tracking is terminated when the next interaction occurs within the detector since that has been taken into account in the unscattered detection probability estimator. The photon-tracking may also be termined by either Russian Roulette or cut-off energy.

After the intensities of γ-rays incident on the detector are predicted by Monte Carlo simulation, the Ge detector response function (Jin *et al.*, 1986) is used to translate this into the complete spectral (pulse-height) response.

6. RESULTS AND DISCUSSION

6.1. Experimental verification

6.1.1. Verification of simulated total pulse height spectrum. Jin *et al.* (1987) made laboratory benchmark tests of the simulated total pulse height spectra generated by their previous Monte Carlo code and got good agreement with experiments in the major prompt γ-ray peaks. However, there are two things which are evident in their results. One is the larger resolution of the experimental spectrum as compared to the simulated spectrum. It is mainly due to the gain and zero shifts for long data acquisition time, and this is a common problem of long term spectrum measurement.

The other is the underestimate of the scattering continuum of the simulated spectrum, which is probably because only the major γ-rays were taken into account in his simulation.

In the present work, the resolution difference is modified by changing the peak resolutions of the detector response function. Also, the scattered γ-ray background disagreement is changed by taking all the available data for prompt γ-rays into account; however, this increases the simulation computer time. Figure 2 shows the comparison between the experimental and the simulated pulse height spectrum of coal sample IV given in Table 4. The disagreement at energies >7 MeV is due to extrapolation of the detector response function beyond the range of its proven validity. It is found that the iron frame (which is not considered in the simulation) used to support the sample box and the detector shielding both make a considerable contribution to the experimental spectra. The elemental analyses of the coal standards were done using proximate analysis and neutron activation analysis. These measurements were made on small samples of the four coals and it is quite likely that there is error in the average sample amounts of several elements. Also the measured values of volatile elements such as Cl, H, etc. can vary significantly from the values for the bulk coal. It is possible that small adjustments in the elemental amounts will give much better agreement between the simulated and the measured spectra (shown in Fig. 2). Considering the fact that the comparison in Fig. 2 is absolute (without any normalization factor), the agreement is considered to be quite good.

6.1.2. Verification of simulated elemental library spectrum. An alternate way of obtaining the elemental library spectra rather than by simulation is by spiking the sample with some known amount of the element of interest (or a compound containing it) and then taking the difference of the measured total γ-ray spectra with and without the spiked amount. The elemental library spectrum of chlorine was obtained by uniformly spiking 0.195% ordinary salt (NaCl) into the sample. Sodium in the salt has little effect in contrast to the chlorine. Figure 3 shows the comparison

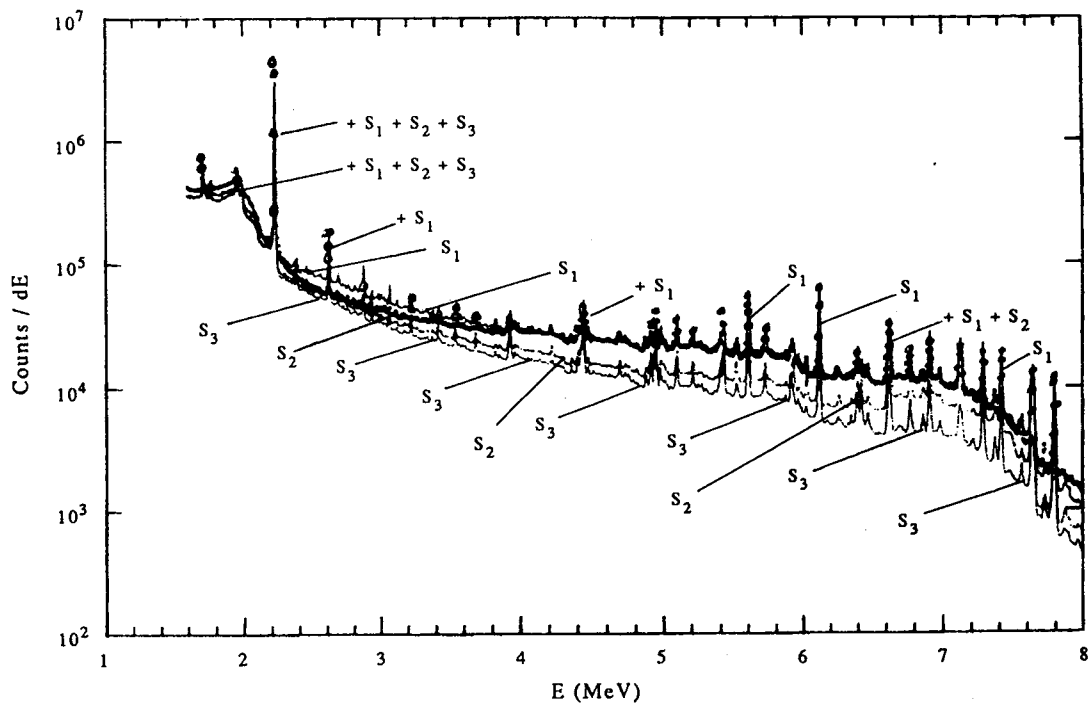

Fig. 2. Comparison between measured and simulated spectra of coal sample IV. ●, Experimental; S_1, simulated +2.841% Fe+0.401% Cl; S_2, simulated +2.841% Fe; S_3, simulated.

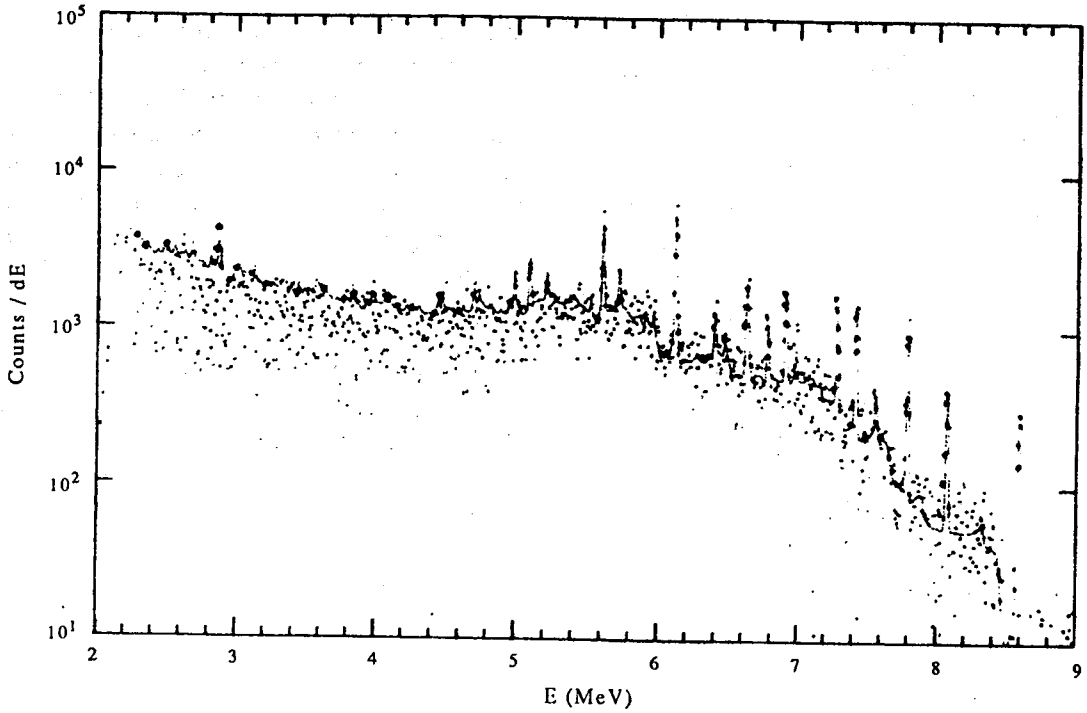

Fig. 3. Comparison between measured and simulated elemental library spectra of chlorine. ●, Measured; —, simulated.

between the experimental and the simulated elemental library spectra of chlorine. It shows good agreement for most of the major peaks. However, there is still some disagreement in some channels which look like peaks in the experimental spectrum. There are several possible reasons for this disagreement. One of them is due to the statistical error in the prompt gamma energy peaks of other elements, which is demonstrated by the peak at 2.224 MeV (due to hydrogen) in the experimental spectrum.

6.2. *Sensitivity of library spectrum shape to sample composition*

After generating the elemental spectra using the detector response function, the elemental library spectra are obtained by dividing the elemental spectra by the atom densities of the corresponding elements. To investigate the sensitivities of library spectrum shapes to the sample composition, these elemental library spectra are normalized first, then the difference distributions are obtained by calculating the relative differences between the normalized elemental library spectra of the 60 *comparison samples*, sample Nos 2 to 61, and those of the *reference sample*, sample No. 1.

Figures 4, 5, and 6 show some of the normalized elemental library spectra and the difference distributions of each element in the sample as well as those of the *extraneous zone**. Based on the information in Figs 4, 5, and 6, the sensitivities of library spectrum shapes of each element in the sample to the concentrations of all the elements in the sample are illustrated in Table 5. It is observed that the shapes of the elemental library spectra are very sensitive to the variation of some elements, such as H, C, O and Ca, while almost insensitive to the variations of other elements, such as Mg, Na, Ti and Cr. To keep valid the assumption that the detector response to the photons from each element is proportional to the concentration (atom density) of that element, both neutron flux distribution and the photon attenuation coefficients of the sample should be kept less affected

* The elemental library spectra of the other elements could be found in Shyu's dissertation.

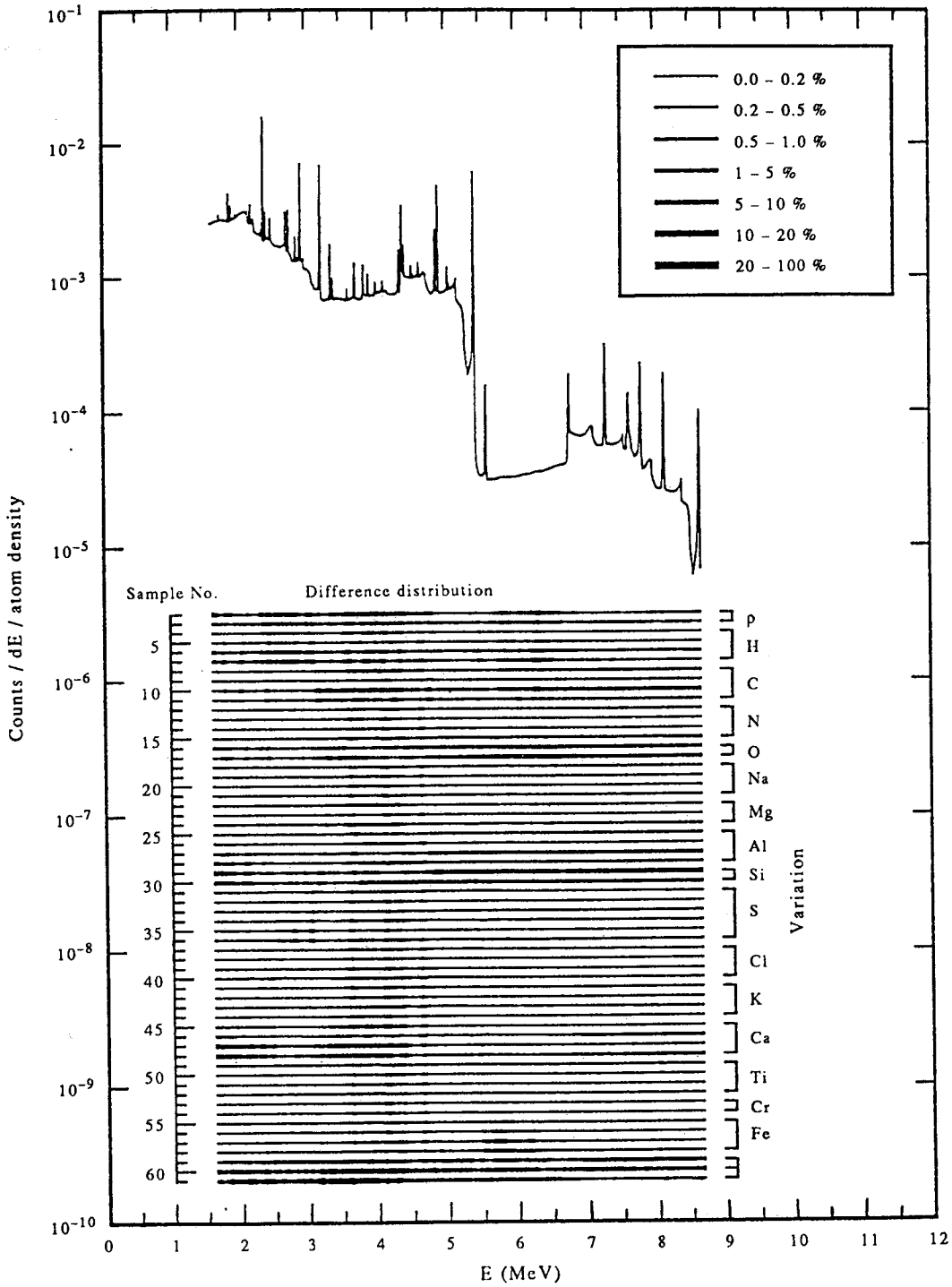

Fig. 4. Simulated elemental library spectrum of S.

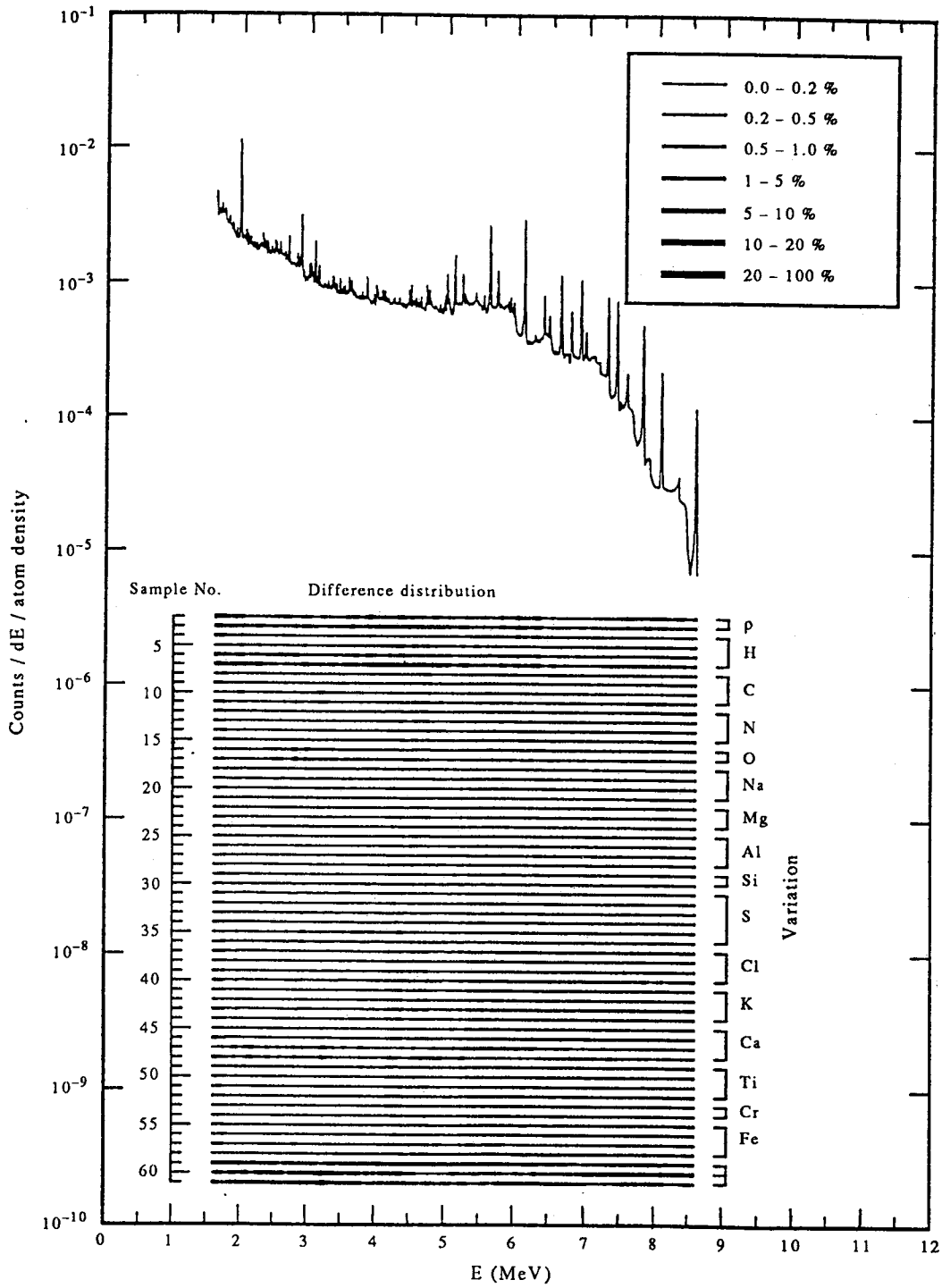

Fig. 5. Simulated elemental library spectrum of Cl.

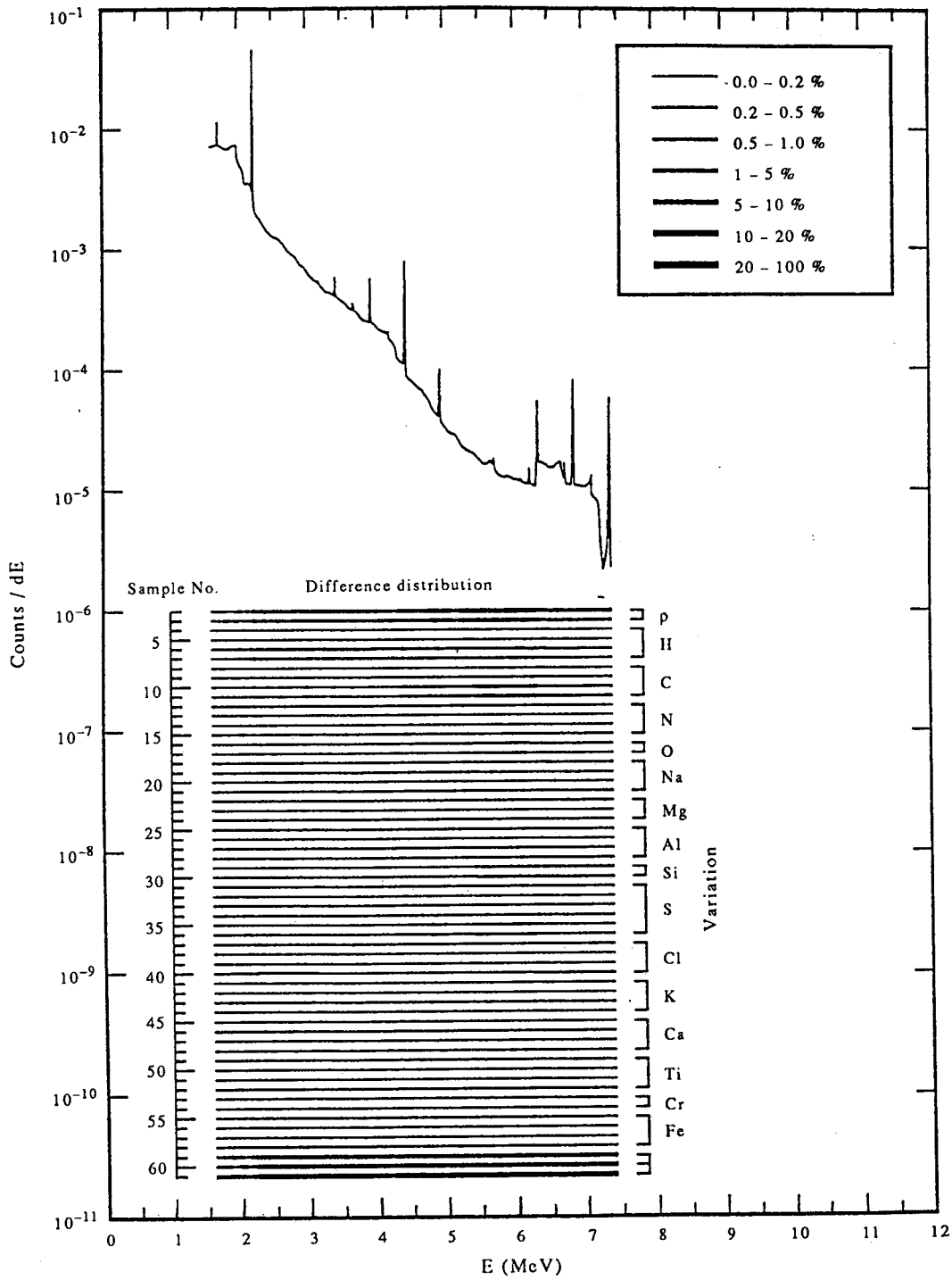

Fig. 6. Simulated library spectrum of extraneous zone.

Table 5. Sensitivity of library spectral shapes of composition variations

Name	Varied element or parameter															
	ρ	H	C	N	O	Na	Mg	Al	Si	S	Cl	K	Ca	Ti	Cr	Fe
H	●	●	◑	○	◑	☆	☆	☆	☆	☆	☆	☆	☆	☆	☆	☆
C	●	●	○	☆	○	☆	☆	☆	☆	☆	☆	☆	○	☆	☆	☆
N	●	●	○	☆	◑	☆	☆	☆	○	○	☆	☆	○	☆	☆	☆
O	●	●	◑	○	○	☆	☆	○	☆	○	☆	☆	○	☆	☆	☆
Na	★	★	◑	◑	●	◑	○	○	◑	○	○	○	◑	○	○	○
Mg	★	★	★	★	●	●	●	●	●	●	◑	●	●	●	●	●
Al	●	◑	◑	☆	◑	☆	☆	◑	☆	☆	☆	☆	●	☆	☆	☆
Si	●	●	○	☆	○	☆	☆	☆	☆	☆	☆	☆	◑	☆	☆	☆
S	●	◑	◑	○	○	☆	☆	○	◑	○	☆	○	◑	☆	☆	○
Cl	◑	◑	○	☆	○	☆	☆	☆	☆	☆	☆	☆	☆	☆	☆	☆
K	◑	◑	☆	☆	○	☆	☆	☆	☆	☆	☆	☆	○	☆	☆	☆
Ca	★	●	○	☆	○	☆	☆	☆	☆	○	☆	☆	●	☆	☆	○
Tl	●	●	○	☆	◑	☆	☆	◑	☆	○	☆	☆	◑	☆	☆	☆
Cr	●	●	●	●	◑	●	◑	◑	◑	●	◑	◑	◑	◑	◑	◑
Fe	●	◑	○	☆	◑	☆	☆	☆	☆	☆	☆	☆	●	☆	☆	☆
Ext.*	◑	○	○	☆	☆	☆	☆	☆	☆	☆	☆	☆	☆	☆	☆	☆

* Ext.: Extraneous Zone.
Notation: ★ ● ◑ ○ ☆ (left to right: Very sensitive to less sensitive).

by the sample composition variations.

1. The neutron macroscopic cross sections*, which govern the reaction probability and thus the neutron flux in the system, differ by orders of magnitude for different elements. Thus, changing the amounts of those elements which have smaller macroscopic cross sections will not appreciably change the neutron flux in the system. On the other hand, if the amounts of those elements which have larger macroscopic cross sections change, the neutron flux in the system will change accordingly. For example, the variation of the chlorine amount only has small effect on the library spectrum shapes even though its microscopic cross section is high, since the atom density of chlorine in the considered sample is very small. While the variation of oxygen amount has larger effect on the neutron flux distribution, than the variation of chlorine amount, even though its microscopic cross section is low, since there is a large amount of oxygen in the considered sample. The variation of hydrogen amount has prominent effects on the neutron flux distribution since both the atom density and the microscopic cross sections of hydrogen are high; on the contrary, the variation of magnesium amount has almost no effect.
2. The attenuation coefficients play an important role in determining the elemental library spectral shapes. Since the attenuation coefficients are functions of energy, prompt γ-rays with different energy will exhibit different attenuation. The hydrogen concentration is the most important one in determining the Compton scattering coefficient of the sample, while the concentrations of heavy elements are more important in determining the pair-production coefficient of the sample†.

Alternatively, the stability of each elemental library spectrum shape can be concluded from Table 5. The elemental library spectrum shapes of chlorine and of iron are very stable to the considered composition variation, while those of magnesium and chromium are very unstable to the composition variation.

* The macroscopic cross section is the product of the microscopic cross section and the atom density of the considered element.

† Compton scattering coefficient $\propto Z/A$, photoelectric effect coefficient $\propto Z^{4.4}/A$, Pair production coefficient $\propto Z^2/A$, where Z is the atomic number and A is the atomic mass number.

6.3. *Elemental analysis sensitivity studies with simulated spectra*

Often one can learn more about a measurement method through simulations than by direct use of experimental data since the normal statistical errors present in the experimental data sometimes tend to obscure the effects of interest. At the present time, interest is primarily focussed on the relationship between the γ-ray intensities and the elemental amounts as a function of sample composition. This is best studied by the use of model simulations.

The library least-squares (LLS) method is tested by using the simulated total pulse height spectrum of the *reference sample*, sample No. 1, as a measured spectrum and using the elemental library spectrum sets of the *comparison samples*, sample Nos 2–58, as the library (standard) spectra, respectively. Tables 6 and 7 show the best and worst cases among all the tested combinations of measured and standard sets. Since the γ-ray intensities are directly proportinal to their *atom densities* (defined as atoms per unit volume), not their weight fractions, the *atom density* of each element is calculated first. The weight fraction of each element is then derived. These results indicate that if we have good first estimates of the amount of major elements (such as hydrogen and carbon), the least-squares method will converge to the right amounts for the other elements (such as chlorine, sulfur and iron), even if the initial guessed amounts of them are far from the true amounts. It should also be noticed that the amounts of some elements, such as oxygen and magnesium, are

Table 6. Result of LLS approach (best case)

Measured data set (M): 1 (density: 0.67552 g/cm^3)
Standard data set (S): 40 (density: 0.67606 g/cm^3)
Reduced chi-square = 2.03E−03

ID	A.D.(M)	A.D.(S)	% diff	L.B.	U.B.	A.D.(C)	% Error
H	2.270E−02	2.270E−02	0	2.000E−02	3.000E−02	2.320E−02	2.04
C	2.160E−02	2.160E−02	0	1.000E−02	4.000E−02	2.180E−02	1.16
N	3.740E−04	3.740E−04	0	3.000E−04	6.000E−04	3.810E−04	1.73
O	4.520E−03	4.520E−03	0	4.000E−03	5.000E−03	4.720E−03	4.23
Na	4.040E−06	4.040E−06	0	1.000E−06	1.000E−05	4.280E−06	5.94
Mg	8.810E−06	8.810E−06	0	1.000E−06	1.000E−05	0.999E−05U	13.45
Al	1.220E−04	1.220E−04	0	5.000E−05	5.000E−04	1.240E−04	1.50
Si	3.770E−04	3.770E−04	0	1.000E−04	1.000E−03	3.830E−04	1.75
S	4.310E−04	4.310E−04	0	1.000E−04	8.000E−04	4.380E−04	1.81
Cl	1.820E−06	1.090E−05	500	1.000E−07	5.000E−05	1.850E−06	1.96
K	2.590E−05	2.590E−05	0	5.000E−06	5.000E−05	2.610E−05	0.58
Ca	3.260E−04	3.260E−04	0	1.000E−04	5.000E−04	3.320E−04	1.77
Ti	4.740E−06	4.740E−06	0	1.000E−06	1.000E−05	4.810E−06	1.53
Cr	9.700E−08	9.700E−08	0	1.000E−08	2.000E−07	9.770E−08	0.71
Fe	9.010E−05	9.010E−05	0	1.000E−05	2.000E−04	9.180E−05	1.84
EZ	1.000E+00	1.000E+00	0	9.000E−01	1.100E+00	1.000E+00	0.00
ID	w/o (M)	w/o (S)	% diff	L.B.	U.B.	w/o (C)	% Error
H	5.62700	5.62254	−0.079	**	**	5.63846	0.20
C	63.63700	63.58661	−0.079	**	**	63.21304	−0.67
N	1.28800	1.28698	−0.079	**	**	1.28670	−0.10
O	17.79200	17.77791	−0.079	**	**	18.20973	2.35
Na	0.02282	0.02280	−0.079	**	**	0.02374	4.03
Mg	0.05263	0.05259	−0.079	**	**	0.05864	11.41
Al	0.81070	0.81006	−0.079	**	**	0.80800	−0.33
Si	2.60000	2.59794	−0.079	**	**	2.59780	−0.08
S	3.39400	3.39131	−0.079	**	**	3.39322	−0.02
Cl	0.01585	0.09502	499.525	**	**	0.01587	0.12
K	0.24940	0.24920	−0.079	**	**	0.24633	−1.23
Ca	3.21655	3.21400	−0.079	**	**	3.21462	−0.06
Ti	0.05581	0.05577	−0.079	**	**	0.05564	−0.30
Cr	0.00124	0.00124	−0.079	**	**	0.00123	−1.11
Fe	1.23700	1.23602	−0.079	**	**	1.23700	0.00

Calculated density (g/cm^3), 0.68792 (Error: 1.83536%).
(M), Measured data set; (S), standard data set; (C), calculated data set; E2, Extraneous Zone; w/o, weight per cent; A.D., atom density (atoms/cm-barn); % Error, [(C)−(M)]/(M)*100%; L.B. and U.B., lower and upper bound constraints.

Table 7. Result of LLS approach (worst case)

Measured data set (M): 1 (density: 0.67552 g/cm³)
Standard data set (S): 2 (density: 0.70930 g/cm³)
Reduced chi-square = 1.69E+00

ID	A.D.(M)	A.D.(S)	% diff	L.B.	U.B.	A.D.(C)	% Error
H	2.270E−02	2.380E−02	5	2.000E−02	3.000E−02	2.200E−02	−3.21
C	2.160E−02	2.260E−02	5	1.000E−02	4.000E−02	2.050E−02	−4.88
N	3.740E−04	3.930E−04	5	3.000E−04	6.000E−04	3.550E−04	−5.23
O	4.520E−03	4.750E−03	5	4.000E−03	5.000E−03	0.400E−02L	−11.59
Na	4.040E−06	4.240E−06	5	1.000E−06	1.000E−05	0.100E−05L	−75.24
Mg	8.810E−06	9.250E−06	5	1.000E−06	1.000E−05	0.100E−05L	−88.65
Al	1.220E−04	1.280E−04	5	5.000E−05	5.000E−04	1.100E−04	−10.07
Si	3.770E−04	3.950E−04	5	1.000E−04	1.000E−03	3.530E−04	−6.15
S	4.310E−04	4.520E−04	5	1.000E−04	8.000E−04	4.050E−04	−5.91
Cl	1.820E−06	1.910E−06	5	1.000E−07	5.000E−05	1.750E−06	−3.78
K	2.590E−05	2.720E−05	5	5.000E−06	5.000E−05	2.060E−05	−20.78
Ca	3.260E−04	3.430E−04	5	1.000E−04	5.000E−04	3.260E−04	−0.14
Ti	4.740E−06	4.980E−06	5	1.000E−06	1.000E−05	3.600E−06	−23.98
Cr	9.700E−08	1.020E−07	5	1.000E08	2.000E−07	1.270E−07	31.24
Fe	9.010E−05	9.460E−05	5	1.000E−05	2.000E−04	8.600E−05	−4.60
EZ	1.000E+00	1.000E+00	0	9.000E−01	1.100E+00	1.040E+00	4.01

ID	w/o (M)	w/o (S)	% diff	L.B.	U.B.	w/o (C)	% Error
H	5.62700	5.62700	0	**	**	5.79687	3.02
C	63.63700	63.63700	0	**	**	64.42769	1.24
N	1.28800	1.28800	0	**	**	1.29921	0.87
O	17.79200	17.79200	0	**	**	16.74333	−5.89
Na	0.02282	0.02282	0	**	**	0.00601	−73.64
Mg	0.05263	0.05263	0	**	**	0.00636	−87.91
Al	0.81070	0.81070	0	**	**	0.77600	−4.28
Si	2.60000	2.60000	0	**	**	2.59723	−0.11
S	3.39400	3.3940	0	**	**	3.39902	0.15
Cl	0.01585	0.01585	0	**	**	0.01623	2.41
K	0.24940	0.24940	0	**	**	0.21030	−15.68
Ca	3.21655	3.21655	0	**	**	3.41873	6.29
Ti	0.05581	0.05581	0	**	**	0.04516	−19.08
Cr	0.00124	0.00124	0	**	**	0.00173	39.69
Fe	1.23700	1.23700	0	**	**	1.25612	1.55

Calculated density (g/cm³), 0.63466 (Error: −6.04815%).
(M), Measured data set; (S), standard data set; (C), calculated data set; E2, Extraneous Zone; w/o, weight per cent; A.D., atom density (atoms/cm-barn); % Error, [(C)−(M)]/(M)*100%; L.B. and U.B., lower and upper bound constraints.

very difficult to determine by LLS. This is as was predicted, since they make a very small contribution to the total spectrum. Thus their amounts should be determined by other methods.

6.4. Feasibility of MCLLS method for poor initial guesses of the major elements

6.4.1. Studies with simulated spectra. It is mentioned in section 6.2 that some major elements, such as H, C, O and Ca, have a stronger effect on changing the library spectrum shapes. Thus the direct application of the LLS method for poor initial guesses of major element amounts cannot guarantee acceptable results since the linearity assumption is no longer valid for this case. However, it is found that the direct application of the LLS method still can converge to the correct composition. This is concluded by using the simulated total spectrum of sample No. 1 as the measured spectrum and using the library spectrum sets of sample Nos 59, 60 and 61, respectively. Table 8 shows the result of using the simulated total spectrum of sample No. 1 as the measured total spectrum and using the library spectrum set of sample No. 60.

6.4.2. Application of MCLLS to experimental spectra. Although the straightforward application of the LLS method appears to be applicable for simulated spectra, several difficulties are encountered

Table 8. LLS result of poor initial guesses of the major elements

Measured data set (M): 1 (density: 0.67552 g/cm³)
Standard data set (S): 60 (density: 0.79314 g/cm³)
Reduced chi-square = 1.63E+01

ID	A.D.(M)	A.D.(S)	% diff	L.B.	U.B.	A.D.(C)	% Error
H	2.270E−02	2.650E−02	16.869	2.000E−02	3.000E−02	2.830E−02	24.82
C	2.160E−02	2.820E−02	30.987	1.000E−02	4.000E−02	2.440E−02	13.14
N	3.740E−04	4.620E−04	23.519	3.000E−04	6.000E−04	4.140E−04	10.58
O	4.520E−03	4.610E−03	1.943	4.000E−03	5.000E−03	0.500E−02U	10.52
Na	4.040E−06	2.470E−06	−38.876	1.000E−06	1.000E−05	0.100E−05L	−75.24
Mg	8.810E−06	8.010E−06	−9.069	1.000E−06	1.000E−05	0.100E−05L	−88.65
Al	1.220E−04	1.940E−04	59.108	5.000E−05	5.000E−04	1.270E−04	3.51
Si	3.770E−04	4.420E−04	17.412	1.000E−04	1.000E−03	4.130E−04	9.69
S	4.310E−04	1.060E−04	−75.445	1.000E−04	8.000E−04	4.910E−04	13.93
Cl	1.820E−06	5.530E−06	203.937	1.000E−07	5.000E−05	2.270E−06	24.86
K	2.590E−05	5.450E−06	−79.003	5.000E−06	5.000E−05	2.070E−05	−20.35
Ca	3.260E−04	2.190E−04	−32.908	1.000E−04	5.000E−04	4.490E−04	37.63
Ti	4.740E−06	5.080E−06	7.187	1.000E−06	1.000E−05	1.050E−06	−77.84
Cr	9.700E−08	9.740E−08	0.368	1.000E−08	2.000E−07	0.200E−06U	106.14
Fe	9.010E−05	1.410E−05	−84.405	1.000E−05	2.000E−04	1.040E−04	15.43
EZ	1.000E+00	1.000E+00	0	9.000E−01	1.100E+00	0.110E+01U	10.00
ID	w/o (M)	w/o (S)	% diff	L.B.	U.B.	w/o (C)	% Error
H	5.62700	5.60100	−0.462	**	**	6.17364	9.71
C	63.63700	70.99500	11.562	**	**	63.28624	−0.55
N	1.28800	1.35500	5.202	**	**	1.25186	−2.81
O	17.79200	15.44800	−13.174	**	**	17.28347	−2.86
Na	0.02282	0.01188	−47.94	**	**	0.00497	−78.23
Mg	0.05263	0.04076	−22.554	**	**	0.00525	−90.02
Al	0.81070	1.09860	35.513	**	**	0.73762	−9.01
Si	2.60000	2.60000	0	**	**	2.50671	−3.59
S	3.39400	0.70980	−79.087	**	**	3.39889	0.14
Cl	0.01585	0.04103	158.864	**	**	0.01740	9.75
K	0.24940	0.04460	−82.117	**	**	0.17461	−29.99
Ca	3.21655	1.83802	−42.857	**	**	3.89120	20.97
Ti	0.05581	0.05095	−8.708	**	**	0.01087	−80.52
Cr	0.00124	0.00106	−14.516	**	**	0.00225	81.19
Fe	1.23700	0.16430	−86.718	**	**	1.25502	1.46

Calculated density (g/cm³), 0.76854 (Error: 13.76961%).
(M), Measured data set; (S), standard data set; (C), calculated data set; E2, Extraneous Zone; w/o, weight per cent; A.D., atom density (atoms/cm-barn); % Error, [(C)−(M)]/(M)*100%; L.B. and U.B., lower and upper bound constraints.

when it is applied to experimental spectra:

1. Statistical errors in the experimental spectrum may obscure the analysis of some elements. For instance, the fractions of elemental spectra of O, Mg and Na are $<0.1\%$ of the total spectrum, while almost all the standard deviations of each channel in the experimental spectra are $>1\%$.
2. The high amplitude of the hydrogen peak at 2.223 MeV tends to obscure the information in the spectrum above that energy since the weight for each channel is a function of the counts in that channel.
3. The high resolution of the Ge detector may become a drawback since minor differences in peak resolution may alter the LLS approach around the peaks.

The first difficulty can be reduced by applying more strict constraints for those elements with extremely low visibilities. This procedure is reasonable since even though the calculated results of those elements meet the applied constraints, it will have a negligible effect on the analysis, except for oxygen, due to their low weight fractions in the sample and low contribution to the measured spectrum. To find an alternate way of applying the LLS method to reduce the second difficulty, the "visibility", which is defined as the fraction of contribution to the measured spectrum, of each

elemental spectrum at different energy intervals is investigated. The results show that (1) some elements have very low visibility in the entire energy range, such as O and Mg, and (2) some elements have very high visibility in some energy ranges but cannot be seen in other energy ranges, for example H and the *extraneous zone*. Since the visibility of each element is so different for different energy ranges, the LLS method can be applied by dividing the energy range into several intervals, and applying the direct (or simple) LLS approach for each interval. The alternative approach is tested by dividing the energy range into three intervals, 1.6–2.27 MeV, 2.27–5 MeV and 5–7 MeV. The LLS approach is first applied to the high energy interval considering only those elements which make a contribution to the spectrum in that interval. It is then applied to the medium energy interval considering all the elements which make a contribution to the total spectrum in that interval, and with strict constraints on the amounts of the elements determined in the high energy interval. Finally, the LLS approach is applied to the low energy interval in a similar way.

The third difficulty can be reduced by using a NaI detector together with a more intense source. In other words, the NaI detector, with high detection efficiency and poor resolution, should be used in practical applications; while the high-purity Ge detector, with much better resolution and poor efficiency, is good for simulation verification purposes. Table 9 shows the result of using the experimental spectrum of sample III as the measured total spectrum and using the library spectrum set of sample No. 1, and dividing the energy range into two intervals, 1.6–2.27 MeV and 2.27–7 MeV. It should be noticed that the true (analyzed) amount of chlorine is lower since some of chlorine was lost during the drying process; besides, the calculated amount of iron is higher since part of it comes from the iron frame of the system. Figure 7 shows a good agreement between the true (measured) and fitted spectra.

6.5. *Guidelines for MCLLS applications*

From the discussion in previous sections, the elemental concentration ranges for giving linear detector response is sample dependent. For the coal samples considered, the hydrogen concentration is the most important one in determining the sample composition range of linear detector response. The algorithm of the iterative MCLLS method should be based on the assumption that the hydrogen concentration is known, from other analytical techniques.

Table 9. Result of LLS approach on experimental spectrum

Measured data set (M): III (density: 0.79314 g/cm^3)
Standard data set (S): 60 (new) (density: 0.67552 g/cm^3)
Reduced chi-square = 3.88E+03

ID	A.D.(M)	A.D.(S)	% diff	L.B.	U.B.	A.D.(C)	% Error
H	2.650E−02	2.270E−02	−14.434	2.000E−02	3.000E−02	2.420E−02	−8.83
C	2.820E−02	2.160E−02	−23.657	1.000E−02	4.000E−02	2.440E−02	−13.42
N	4.620E−04	3.740E−04	−19.041	3.000E−04	6.000E−04	0.600E−03U	29.84
O	4.610E−03	4.520E−03	−1.906	4.000E−03	5.000E−03	0.400E−02L	−13.27
Na	2.470E−06	4.040E−06	63.602	1.000E−06	1.000E−05	0.100E−05L	−59.49
Mg	8.010E−06	8.810E−06	9.973	1.000E−06	1.000E−05	0.100E−05L	−87.51
Al	1.940E−04	1.220E−04	−37.149	5.000E−05	5.000E−04	4.270E−04	119.45
Si	4.420E−04	3.770E−04	−14.83	1.000E−04	1.000E−03	7.520E−04	70.16
S	1.060E−04	4.310E−04	307.253	1.000E−04	8.000E−04	1.220E−04	14.96
Cl	5.530E−06	1.820E−06	−67.098	1.000E−07	5.000E−05	1.100E−05	98.61
K	5.450E−06	2.590E−05	376.266	5.000E−06	5.000E−05	1.860E−06	240.56
Ca	2.190E−04	3.260E−04	49.049	1.000E−04	5.000E−04	3.420E−04	56.29
Ti	5.080E−06	4.740E−06	−6.705	1.000E−06	1.000E−05	0.100E−04U	96.82
Cr	9.740E−08	9.700E−08	−0.367	1.000E−08	2.000E−07	0.200E−06U	105.39
Fe	1.410E−05	9.010E−05	541.24	1.000E−05	2.000E−04	9.710E−05	591.00
EZ	1.000E+00	1.000E+00	0	9.000E−01	1.100E+00	0.900E+00L	−10.00
BG	1.000E+00	1.000E+00	0	9.000E−01	1.10E+00	0.900E+00L	−10.00

Calculated density (g/cm^3), 0.74348 (Error: −6.26140%).
(M), Measured data set; (S), standard data set; (C), calculated data set; E2, Extraneous Zone; (BG), background; w/o, weight per cent; A.D., atom density (atoms/cm-barn); % Error, [(C)−(M)]/(M)*100%; L.B. and U.B., lower and upper bound constraints.

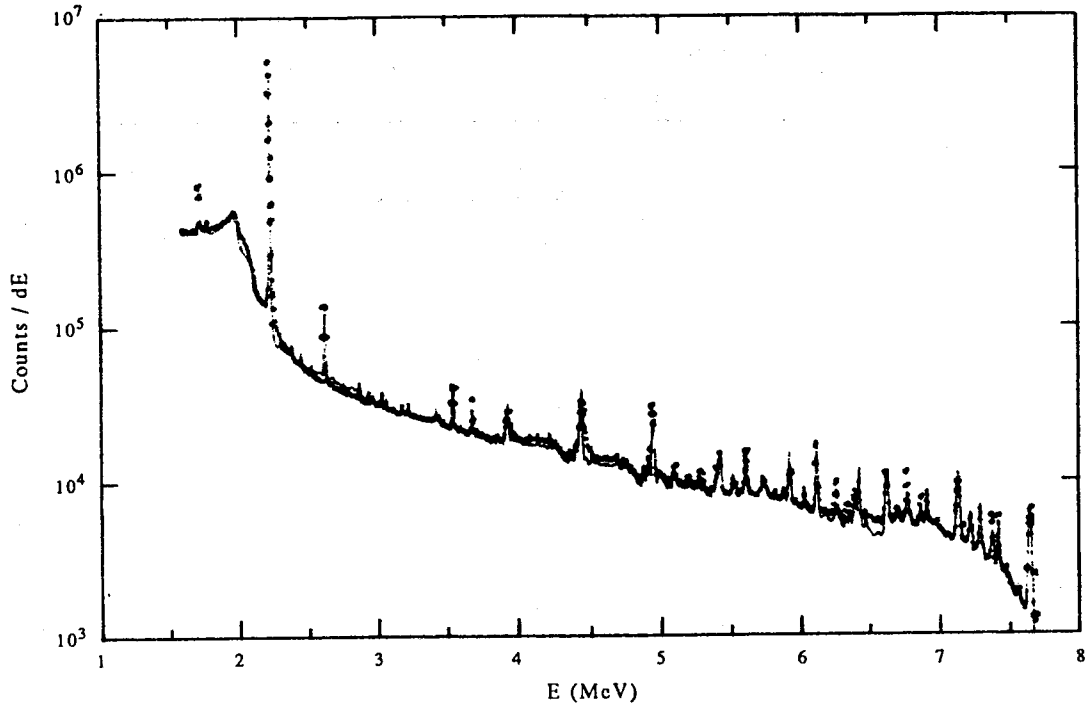

Fig. 7. Comparison between experimental and fitted spectra of coal sample III. ●, Measured; —, fitted.

Another set of elemental library spectrum set is simulated by adjusting the calculated hydrogen concentration in Table 8 to the true hydrogen concentration and using the calculated concentrations for the other elements. The result of reapplying the LLS method with the new library spectrum set is tabulated in Table 10, which shows better results.

The main drawback of the Monte Carlo simulation method is that it often takes very long to make the simulation converge to the desired accuracy. Thus, the practical application of the iterative MCLLS method should use the following guidelines:

1. For a specific kind of sample, it is necessary to determine the important elements which affect either the neutron macroscopic cross sections or the photon attenuation coefficients of the sample.
2. Use the Monte Carlo simulation method to build library spectrum sets based on the variation of those important elements.
3. Find a way to obtain as good an initial guess of the concentrations of these important elements as possible.
4. Choose a proper library spectrum set to apply the LLS method.
5. If the chosen library set does not give a reasonable result, choose another set and reapply the LLS method until it does.

7. SUMMARY AND CONCLUSIONS

The major objective of this research was to investigate the implementation of the Monte Carlo–Library Least-Squares approach to the analysis of bulk coal by neutron capture γ-ray analysis. This was carried out by using Monte Carlo simulation to generate pulse height spectra for a multiple number of coal samples consisting of 15 elements with known elemental concentrations. The simulation also generated library spectra from each of the elements for an assumed set of sample composition and from the γ-rays that are produced extraneous to the sample. The

Table 10. Result of iterative MCLLS method

Measured data set (M): 1 (density: 0.67552 g/cm³)
Standard data set (S): 60 (new) (density: 0.75915 g/cm³)
Reduced chi-square = 7.52E+00

ID	A.D.(M)	A.D.(S)	% diff	L.B.	U.B.	A.D.(C)	% Error
H	2.270E−02	2.270E−02	0.123	2.000E−02	3.000E−02	2.410E−02	5.95
C	2.160E−02	2.440E−02	13.143	1.000E−02	4.000E−02	2.470E−02	14.41
N	3.740E−04	4.140E−04	10.578	3.000E−04	6.000E−04	3.880E−04	3.66
O	4.520E−03	5.000E−03	10.518	4.000E−03	5.000E−03	0.400E−02L	−11.59
Na	4.040E−06	1.000E−06	−75.222	1.000E−06	1.000E−05	0.100E−04U	147.63
Mg	8.810E−06	1.000E−06	−88.651	1.000E−06	1.000E−05	0.100E−04U	13.55
Al	1.220E−04	1.270E−04	3.514	5.000E−05	5.000E−04	1.260E−04	3.38
Si	3.770E−04	4.130E−04	9.688	1.000E−04	1.000E−03	3.790E−04	0.50
S	4.310E−04	4.910E−04	13.934	1.000E−04	8.000E−04	4.610E−04	6.95
Cl	1.820E−06	2.270E−06	24.896	1.000E−07	5.000E−05	1.830E−06	0.43
K	2.590E−05	2.070E−05	−20.347	5.000E−06	5.000E−05	3.280E−05	26.45
Ca	3.260E−04	4.490E−04	37.633	1.000E−04	5.000E−04	3.140E−04	−3.94
Ti	4.740E−06	1.050E−06	−77.841	1.000E−06	1.000E−05	5.780E−06	21.98
Cr	9.700E−08	2.000E−07	106.438	1.000E−08	2.000E−07	1.210E−07	24.94
Fe	9.010E−05	1.040E−04	15.427	1.000E−05	2.000E−04	9.340E−05	3.70
EZ	1.000E+00	1.000E+00	0	9.000E−01	1.100E+00	1.040E+00	3.76
ID	w/o (M)	w/o (S)	% diff	L.B.	U.B.	w/o (C)	% Error
H	5.62700	5.01324	−10.907	**	**	5.52989	−1.73
C	63.63700	64.06894	0.679	**	**	67.53604	6.13
N	1.28800	1.26734	−1.604	**	**	1.23840	−3.85
O	17.79200	17.49722	−1.657	**	**	14.59157	−17.99
Na	0.02282	0.00503	−77.951	**	**	0.05242	129.70
Mg	0.05263	0.00531	−89.901	**	**	0.05543	5.32
Al	0.81070	0.74674	−7.889	**	**	0.77739	−4.11
Si	2.60000	2.53771	−2.396	**	**	2.42383	−6.78
S	3.39400	3.44093	1.383	**	**	3.36718	−0.79
Cl	0.01585	0.01762	11.137	**	**	0.01477	−6.84
K	0.24940	0.17677	−26.122	**	**	0.29254	17.30
Ca	3.21655	3.93932	22.47	**	**	2.86606	−10.90
Ti	0.05581	0.01100	−80.282	**	**	0.06315	13.14
Cr	0.00124	0.00228	83.696	**	**	0.00144	15.89
Fe	1.23700	1.27054	2.712	**	**	1.18991	−3.81

Calculated density (g/cm³), 0.72826 (Error: 7.80671%).
(M), Measured data set; (S), standard data set; (C), calculated data set; E2, Extraneous Zone; w/o, weight per cent; A.D., atom density (atoms/cm-barn); % Error, [(C)−(M)]/(M)*100%; L.B. and U.B., lower and upper bound constraints.

library spectra contained the effect of nonlinearities in the sample spectrum and were, therefore, appropriate for use in a linear library least-squares search for the elemental concentrations. The searched concentrations could be compared to the known values used to compute the sample pulse height spectrum to determine the validity of the MCLLS method. The basic questions to be settled were: (1) the accuracy of the Monte Carlo simulation of the sample spectrum and of the library elemental spectra, (2) the convergence of the searched elemental concentrations to the true values, and (3) identification of the problems which may arise in the implementation of the MCLLS scheme to actual analysis problems involving experimentally measured sample spectra.

To settle the first question, four bulk samples of coal were obtained and were characterized using neutron activation analysis and proximate analysis. Laboratory data on the capture γ-ray pulse height spectra were collected on the four bulk samples using a high resolution Ge detector. A Monte Carlo program written by Jin (his thesis) was modified for improvements in accuracy and run time. This code was used to generate the simulated spectrum for each of the four coal sample compositions and these spectra were compared to the measured spectra. The spectra agreed very well over the range of 1.5 to about 7.5 MeV which is approximately the range over which the detector spectral response function that is used if the simulation is valid. The simulated library spectrum of chlorine for one of the coal samples was compared to a chlorine library spectrum

measured by spiking the coal with salt. The agreement was deemed excellent and adequate for investigating the MCLLS method.

To study the second question, simulations of sets of library spectra were carried out with assumed elemental concentrations which were different from the actual concentrations by up to a few percent for each of the elements. This could be done efficiently using the correlated sampling option in the Monte Carlo program. Using different sets of the simulated library spectra, a constrained least-squares search was applied on a sample spectrum that was simulated using the known elemental concentrations. The comparisons of the searched values to the actual concentrations showed various important aspects of the MCLLS approach:

1. Certain elements are much more sensitive in their library spectrum shapes to the presence of other elements. Table 5 shows the sensitivity matrix of the 15 elements to variations in their elemental concentrations. This information could serve as a guideline in determining which of the elements must be known with the highest accuracy in the initial estimates for the least-squares search.
2. Hydrogen and carbon must be known with the highest accuracy if the least-squares method is to converge to the correct values for the other major elements of environmental consequence such as chlorine, sulfur and iron. In fact, it is recommended that hydrogen and carbon should be determined by other analytical methods such as microwave measurements and inelastic neutron scattering.
3. Certain elements such as magnesium and oxygen probably cannot be determined correctly by PGNAA since they make little contribution to the total sample spectrum. The concentration of oxygen is significant in coal, but its effect on the spectrum is primarily through the scattering of neutrons and not through capture.

For the study of the third basic question, the measured spectra of the four coal samples were analyzed by MCLLS. The following problems were identified:

1. Statistical errors, pulse pile-up distortions and gain fluctuations in the counting equipment can cause the experimental spectrum to be different from the simulated library spectra and introduce significant errors in the least-squares search. O, Mg and Na are particularly notorious in having statistical uncertainties since their contribution to the total spectrum is $<0.1\%$ in each case. On-line analyzers must use high counting rates since the analysis time is short. This can result in pulse pile-up which must be minimized by either hardware, software or both. Also, gain fluctuations must be guarded against since they can increase the resolution of the spectrometer and also shift the peaks in the spectrum.
2. The hydrogen peak at 2.223 MeV in coal is so large that it tends to decrease the sensitivity of the LLS analysis for other elements, most of which contribute to the spectrum at energies higher than that of hydrogen. A regionwise search of the measured spectrum starting with a high energy portion is proposed in section 6.4.2 and appears to be feasible. An alternative way is to use a different weighting function (instead of $1/\sigma_i^2$) in applying LLS approach in order to reduce the hydrogen peak effect.
3. The high resolution of the Ge detector can be a drawback in MCLLS analysis since minor changes in the peak resolution due to detector degradation or gain fluctuations can introduce significant inaccuracies in the fits around the peaks. NaI detectors appear to have an advantage in this regard.

The advantages of the MCLLS approach over conventional analysis algorithms are:

1. The interelement effects are automatically taken into account in the MCLLS approach if the initial estimate of the sample composition is fairly close to the actual.

2. It uses all of the information that is present in the experimental data.
3. Determination of library spectra through experiments is a very expensive process and it is avoided entirely in the MCLLS approach.
4. Library spectra of any sample composition can be obtained.
5. The problems associated with spectra subtraction are avoided.
6. It gets elemental spectra for all the considered elements, including those minor contribution elements, such as O and Mg, which are almost impossible to obtain experimentally.

The following recommendations are made for future work:

1. Study of other feasible variance reduction techniques: It takes about 15 CPU hours to run the present code on a DEC station 3100 for the variances of the unscattered prompt γ-rays from the sample to converge to about 15%. Since all of the prompt γ-rays of all the elements in the interaction size zone are forced to be emitted when radiative capture occurs, lots of computer time is used to evaluate the unscattered detection probabilities given in equation (8). For the coal sample, there are totally 1452 prompt γ-rays being considered. Instead of applying the deterministic estimator 1452 times when radiative capture occurs in the sample, one can first discretize the gamma energy range into several intervals, say 14 intervals, and compute the unscattered detection probabilities at these mesh energys. Then the unscattered detection probabilities of those 1452 prompt γ-ray energies can be evaluated either by using the function obtained by fitting those 14 probabilities as a function of γ-ray energy or by interpolation. This procedure should save about 99% of the CPU time of applying the deterministic estimator when radiative capture occurs in the sample.

2. Effect of neutron absorber on the shapes of library spectra: The existence of neutron absorbers, such as B which do not produce a library spectrum, will change the neutron flux in the system and thus the radioactive capture interaction rate distribution in the system. Furthermore, the shapes of library spectra will change accordingly.

3. Application of MCLLS to other configurations: Besides the transmission configuration, analyzers in other configurations such as backscattering geometry or borehole geometry, can be studied in a similar way when the MCLLS method is applied to these configurations.

REFERENCES

Armstrong S. B. (1965) The energy-dependent total neutron cross section. *Nucl. Sci. Eng.* **23**, 192.

Beyster J. R., Antunez, H. and Brouwer W. (1965) Integral neutron thermalization, Annual Summary Report (Oct. 1, 1964–Sept. 30, 1965), Report GA-6824, General Atomic Company.

Booth T. E. (1989) Zero-variance solutions for linear Monte-Carlo. *Nucl. Sci. Eng.* **102**, 332.

Carter L. L. (1977) Version of MCNP to Treat Perturbations. Office Memorandum, Los Alamos Scientific Laboratory, July 14.

Carter L. L. and Cashwell E. D. (1955) Particle-transport simulation with the Monte Carlo method. Energy Research and Development Administration Critical Review Series, TID-26607, U.S. Department of Energy, Oct. 1975.

Dejonghe G. *et al.* (1980a) Study of perturbations using correlated Monte Carlo method. ORNL/RSIC-44, Oak Ridge National Laboratory.

DeJonghe G., Gonnard J. and Nimal J. C. (1980b) Studies of perturbations using correlated Monte Carlo. ORNL/RSIC-44, Oak Ridge National Laboratory 63–93

Duffey D., Cox S. A., Herzenberg C. L., O'Fallon N. M. and Wiggins P. F. (1978) Coal analytical assembly using capture gamma rays from accelerator neutrons. *Trans. Am. Nucl. Soc.* **30**, 142.

Everett C. J. and Cashwell E. D. (1970) Approximation for the inverse of the Klein–Nishina probability distribution. Report LA-4448.

Everett C. J., Cashwell E. D. and Turner G. D. (1971) On a new method of sampling the Klein–Nishina probability distribution for all incident photon energies above 1 keV. Report LA-4663.

Gardner R. P. and Verghese K. (1971) On the solid angle subtended by a circular disc. *Nucl. Instrum. Methods* **93**, 163.

Gardner R. P. and Wielopolski L. (1977) A generalized method for correcting pulse-height spectra for peak pile-up effect due to double sum pulses. *Nucl. Instrum. Methods* **140**, 289.

Gardner R. P., Choi H. K., Michael M. W., Yacout A. M., Jin Y. and Verghese K. (1987) Algorithms for forcing scattered radiation to spherical, planar circular, and right circular cylindrical detectors for Monte Carlo simulation. *Nucl. Sci. Eng.* **95**, 245.

Gardner R. P., Michael M. W., Towsley C. W., Shyu C. M. and Verghese K. (1990) Correlated sampling in the McDNL and McPNL codes for neutron and neutron lifetime log corrections. *IEEE Transact. Nucl. Sci.* **37(3)**, 1360.

Gozani T., Elias E., Orphan V., Reed J. and Shreve D. (1977) Prompt-neutron activation analysis—applications to coal analysis. *Trans. Am. Nucl. Soc.* **26**, 160.

Gozani T., Bozorgmanesh H., Brown D., Elias E., Maung R. and Reynolds G. (1978) Coal elemental analysis by prompt-neutron activation analysis. *Trans. Am. Nucl. Soc.* **28**

Hall M. C. G. (1980a) Monte Carlo perturbations theory in neutron transport calculations. ORNL/RSIC-44, Oak Ridge National Laboratory.

Hall M. C. G. (1980b) Monte Carlo perturbations theory in neutron transport calculations. ORNL/RSIC-44, Oak Ridge National Laboratory, 47–62.

Huffman Laboratory, Inc., Private Communication, Golden, Colorado (1988).

Jin Y., Gardner R. P. and Verghese K. (1987) A Monte Carlo model for the complete pulse-height spectral response of neutron capture prompt γ-ray analyzers for bulk media and borehole configurations. *Nucl. Geophys* **1**, 167.

Jin Y., Gardner R. P. and Verghese K. (1986) A semi-empirical model for the gamma-ray response function of germanium detectors based on fundamental interaction mechanisms. *Nucl. Instrum. Methods* **A242**, 416–426.

Kinsey R. (ed.) (1979) ENDF/B Summary Documentation, BNL-NCS-17541 (ENDF-201), 3rd Edn (ENDF/B-V). National Nuclear Data Center, Brookhaven National Laboratory.

Lone M. A., Leavitt R. A. and Harrison D. A. (1981) Prompt gamma rays from thermal-neutron capture. *At. Data Nucl. Data Tables* **26**, 511 (1981).

Marshall III J. H. and Zumberge J. F. (1989) On-line measurements of bulk coal using prompt gamma neutron activation analysis. *Nucl. Geophys.* **3**, 445.

McGrath E. J. and Irving D. C. (1975) *Techniques for Efficient Monte Carlo Simulation*, Vol. III, Variance Reduction, ORNL-RSIC-38 (Vol. III). Oak Ridge National Laboratory, Oak Ridge, Tennessee.

Prettyman T. H. (1990) HERMETOR: a modular geometric modeller for particle tracking in specific purpose Monte Carlo codes. Version A Manual, North Carolina State University, Raleigh, North Carolina.

Rainwater L. J., Havens Jr W. W., Dunning J. R. and Wu C. S. (1948) Slow neutron velocity spectrometer studies of H, D, F, Mg, S, Si, and quartz. *Phys. Rev.* **73**, 733.

Reynolds G., Bozorgmanesh H., Elias E., Gozani T., Maung T. and Orphan V. (1979) *Nuclear Assay of Coal*—Vol. I, Coal Composition by Prompt Neutron Activation Analysis—Basic Experiments. Report EPRI FP-989, Vol. 1 (1979).

Shyu C. M., He T., Verghese K. and Gardner R. P. (1988) Monte Carlo–library least-squares principle for nuclear analyzers. *Trans. Am. Nucl. Sci.* **56**, Supplement No. 44.

Storm E. and Israel H. I. (1967) Photon cross sections from 0.001 to 100 MeV for elements 1 through 100. Report LA-3753.

Verghese K., Gardner R. P., Michael M., Shyu C. M. and He T. (1988) The Monte Carlo–library least square analysis principle for borehole nuclear well logging elemental analyzers. *Nucl. Geophys.* **2**, 183

Weaver J. N. Private Communication, Nuclear Energy Services, North Carolina State University, Raleigh, North Carolina (1989).

Yakowitz S. J. (1977) *Computational Probability and Simulation.* Addison-Wesley Inc., Reading, Massachusetts (1971).

Yuan Y. L., Gardner R. P. and Verghese K. (1987) A Monte Carlo model for on-line neutron capture prompt gamma-ray analysis of coal in transmission geometry. *Nucl. Techn.* **77(1)**, 97.